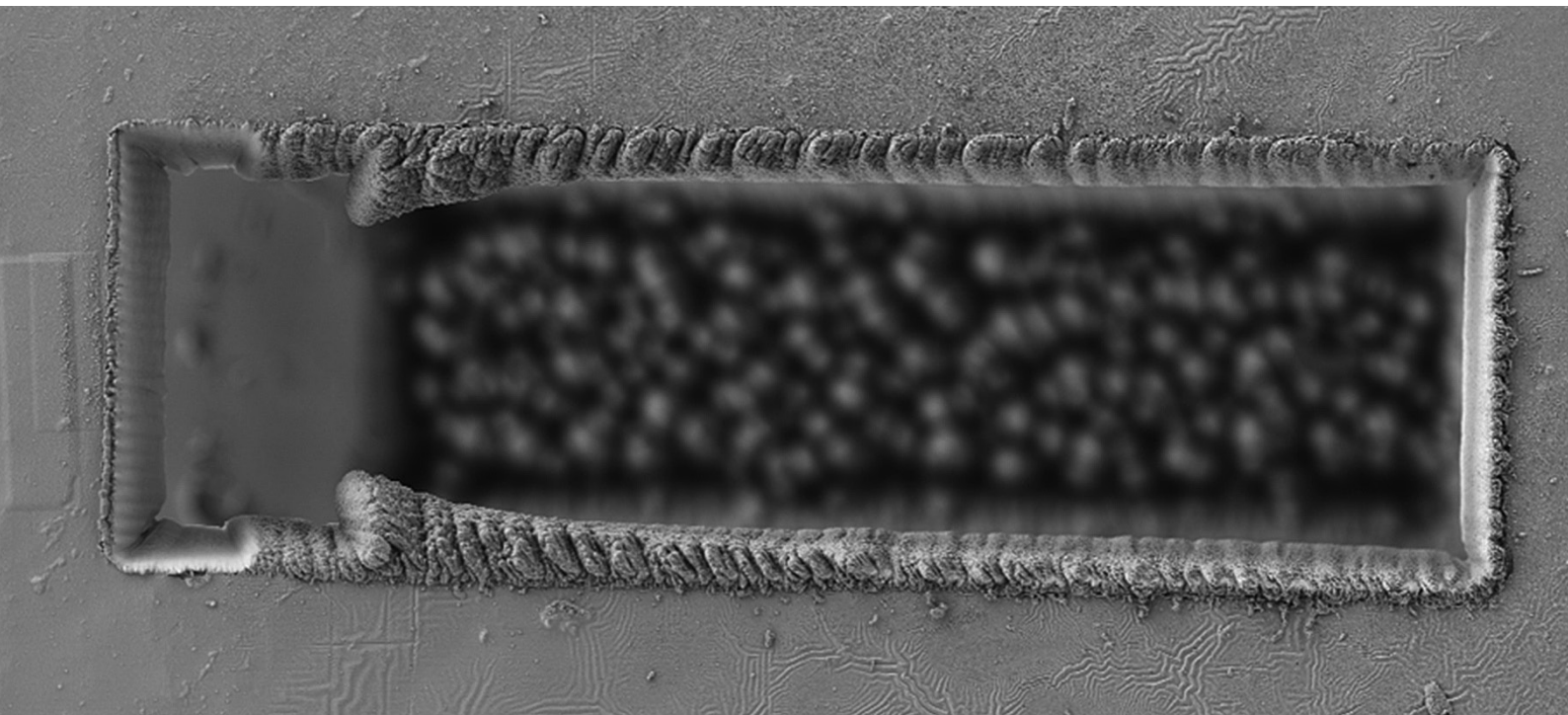


Hitting Defects Accurately Through Correlation: A Case Study of Sparse-Particle Analysis in a Bulk Material



Hitting Defects Accurately Through Correlation: A Case Study of Sparse-Particle Analysis in a Bulk Material

Abstract

How can sparse micron-sized defects or anomalous particles, buried within millimeters of an otherwise homogenous material matrix, be accurately identified and analyzed in an efficient way? This note describes a case study of a 3D correlative workflow using non-destructive 3D X-ray microscopy (XRM) to identify the presence and location of sparse anomalous particles, after which a focused ion beam scanning electron microscope (FIB-SEM) equipped with an integrated femtosecond (fs) laser is used to access the region of interest (ROI), prepare a cross section through the identified particles, and perform EDS to determine their composition. It is demonstrated for this use case that the entire workflow can be applied within a single day.

Introduction

It is important to understand defects or impurities hidden within a bulk material for materials research, process development, reliability, and quality control.

In this case study, materials characterization was required for a small iron plate with approximate dimensions 12 mm x 12 mm x 0.3 mm. This iron plate was removed from a batch suspected to have possible anomalous particles located within its bulk. Particles are a concern because they can serve as crack initiation sites. The characterization goal was to first determine whether such anomalous particles existed, and if so, to determine their elemental composition to aid determination of the manufacturing process step giving rise to the particles. Characterization of the iron plate was carried out using a 4-step workflow as summarized in Figure 1. This workflow is known as the Cut2ROI (cut to region-of-interest) workflow and uses ZEISS Versa 3D XRM and ZEISS Crossbeam laser FIB-SEM, along with Atlas 5 correlative software installed on the Crossbeam.



Figure 1 Summary of the four main steps of the Cut2ROI workflow used in this study. Step 1 is performed using ZEISS Versa 3D X-ray microscopy, and Steps 2 through 4 are performed using ZEISS Crossbeam laser FIB-SEM.

Microscopy Methods

To understand the instruments used in this study, brief summaries are provided below.

3D X-ray microscope (XRM): The first step of the workflow applies a ZEISS Xradia Versa 3D X-ray microscope [1]. Data acquisition is performed by automated radiographic imaging of a sample at many angles of rotation. Radiographs are computationally reconstructed into a 3D volume by conventional FDK or Deep Learning algorithms, producing a visualization of internal features non-destructively. This case study implemented conventional FDK algorithms for reconstruction. In contrast to microCT, 3D XRM uses an optically-coupled scintillator design to deliver 'Resolution-at-a-Distance' with submicron-scale spatial resolution even within relatively large samples [2]. Compared to electron microscopy-based approaches, limitations still exist regarding 3D XRM spatial resolution or contrast and these motivate the use of a correlative approach to investigate smaller length scales with FIB-SEM.

Before initiating a 3D XRM scan for correlated microscopy, surface features must be identified or created that are visible in all the desired imaging modalities, and the 3D XRM scan must be done to include these surface fiducials within the volume scanned. If the sample does not contain native surface fiducials, then fiducials can be created by placing TEM finder grids on the sample, or by mechanical, FIB or laser marking [3-5].

Focused ion beam scanning electron microscopy (FIB-SEM) with integrated fs-laser: To perform the targeted LaserFIB milling on a sample imaged by XRM, the sample stub was mounted onto the Crossbeam laser sample holder and loaded into the main chamber of a ZEISS Crossbeam FIB-SEM instrument with a fs laser (TRUMPF SE + Co. KG, Ditzingen, Germany, wavelength 515 nm, pulse length <350 fs, pulse repetition rate of 1 kHz to 1 MHz, focus spot diameter <15 μm) coupled into a processing chamber attached to the instrument's airlock [6]. The sample holder enables milling target coordinate transfer between the SEM and the laser by registering four reference marks on the holder both in the SEM and in the laser reference frames. While a FIB-SEM combines the strengths of nm-scale imaging/analytics with the ability to access site-specific locations beneath the surface, the milling rates achievable with a FIB limit the volume of material that can be removed in a practical timeframe to depths on the order of ~50-100 μm for Ga⁺ ions, and several hundred μm for Xe⁺ ions. The recent integration of a fs-laser ablation system on the ZEISS Crossbeam overcomes this constraint by extending the material removal capability to much deeper (mm) and faster (seconds to minutes) dimensions, while also serving as the critical bridge between the XRM and FIB-SEM techniques in the Cut2ROI workflow.

The patented architecture of a FIB-SEM integrated laser having its own process chamber ensures ablated by-products do not contaminate sensitive detectors or degrade the high vacuum of the main chamber that is required for high-resolution imaging. Thus, efficient sample preparation and analysis are enabled while maintaining a pristine imaging chamber. For volumes in the range of 0.5 to 10 cubic millimeters, an inert gas cross-jet can be activated beneath the protective glass below the laser window. This ensures the optical path is kept free of recast debris and provides consistent ablation rates, reduced optical path maintenance, and longer runtimes in a single uninterrupted session. This in turn enables reliable results, improved efficiency and consistency, and opportunities for automated workflows.

Results

Successful data correlation, region of interest targeting, and analysis across the different imaging modalities of 3D XRM, SEM, and EDS was achieved. Details and results for each step of the Cut2ROI workflow are described below.

Step 1 - Identify: The iron plate was mounted onto a pin and scanned twice using the standard Scout and Zoom workflow in the Versa 3D X-ray microscope. The Scout and Zoom workflow provides a large field-of-view (LFOV) survey scan to look for interesting features, followed by a high-resolution, smaller field-of-view scan at a target location identified in the first survey scan. ZEISS Versa's control system and 'Resolution-at-a-Distance' performance allows switching from LFOV to high-resolution scanning without needing to re-mount the sample or downsize it to produce a high-resolution interior tomography dataset.

The conditions used for the two 3D XRM scans are as follows:

1. The LFOV scan was acquired in ~40 minutes using the 0.4X objective lens at 70kV/8.5 watts and 14.21 μm voxel resolution
2. The high-resolution interior tomography scan was acquired in approximately 1 hour using the 4X objective lens at 80kV/10 watts and voxel size of 1.38 μm .

Three native surface fiducials were identified in suitable areas prior to initiating any of the scans. The selected fiducials in this case consisted of two corners of the sample and a pre-existing FIB milled box.

The resulting reconstructed 3D XRM data volume is visualized in Figure 2. Orthogonal virtual cross sections are used to quickly explore the data and locate features of interest..

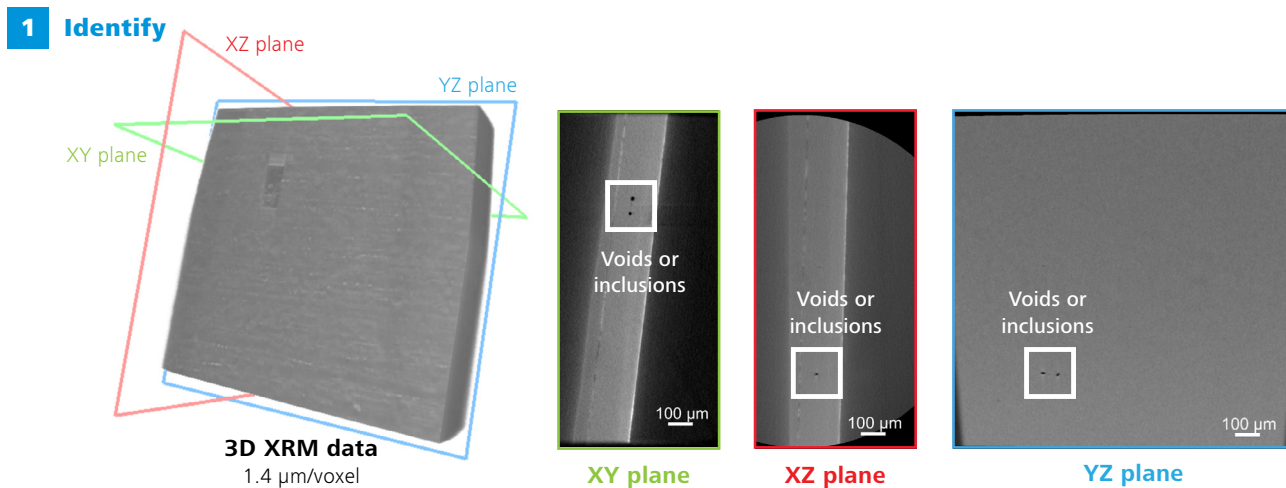


Figure 2 Virtual cross sections from 3D XRM data are used to visually identify the presence and location of two anomalous features within the Fe bulk matrix. These anomalies are located approximately 100 μm beneath the sample surface.

In this sample, two anomalous features were found, separated by about 40 μm and located approximately 100 μm beneath the surface. The 3D XRM data confirms that these features have lower densities compared to the main matrix, but does not reveal their composition. Thus, while the 3D XRM data confirms the presence of anomalies that could be indicative of particles, and provides a useful guide, other techniques are required to fully characterize the anomalies contained in this region of interest. The anomalies are small and would be difficult to accurately cross section using mechanical polishing and broad ion beams. Therefore, a decision was made to apply the fs-laser and a FIB polish using ZEISS Crossbeam laser FIB-SEM.

To perform a fs-laser assisted FIB-SEM cross-section, the FIB analyst had to relocate and identify these same buried features to accurately place the laser and FIB cuts. This was done in the Crossbeam aided by 3D XRM data and Atlas 5 correlative software. First, the sample was mounted onto an SEM stub and loaded into the FIB-SEM main chamber. To start the correlation, the 3D XRM data volume was imported into the Atlas 5 software residing on the FIB-SEM, and an SEM image of the top surface of the sample was acquired from the area that is also captured within the 3D XRM data volume. Spatial registration of the 3D XRM data to the 2D SEM surface view was performed in Atlas 5 by pixel scaling, data rotation, and data translation to align native fiducials on the sample surface that are visible with both modalities. Two corners of the sample along with a pre-existing FIB milled box served as the fiducials in this case. Once the correlation on the surface was anchored, the X-ray volume was virtually sliced by scrolling through the X-ray volume along the direction perpendicular to the sample surface until the features of interest were identified. By comparing the SEM top surface with the virtual slice of the X-ray data, the location of the features was easily identified. Note that while sufficient natural fiducials exist in this case, in the event of a smooth

featureless surface, fiducials can be introduced using a variety of methods prior to step 1 of the workflow, as referenced earlier in the methods section.

Step 2 - Access: With the surface (SEM) and sub-surface (XRM) appropriately registered in 3D space, the SEM and fs-laser system coordinates were registered using fiducials built into the Crossbeam laser FIB-SEM sample holder. Then the fs-laser was used to dig a trench adjacent to the buried features of interest (Figure 3a), providing access to the target site for further refined work and analysis. Laser ablation was performed with optimized laser parameters for 10 minutes, over a volume of $\sim 650 \mu\text{m L} \times 175 \mu\text{m W} \times 180 \mu\text{m D}$, in a 3-step cutting process as follows:

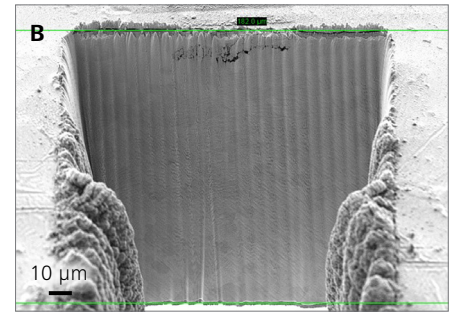
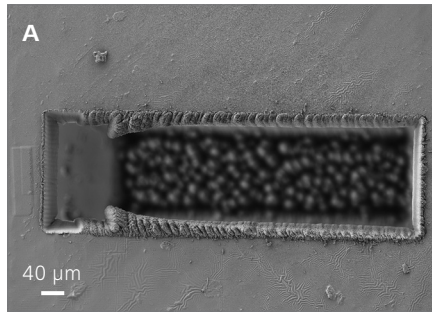
1. Laser power 100%, pulse frequency of 300 kHz, scan speed of 950 mm/s for 26 seconds
2. Laser power 26%, pulse frequency of 12 kHz, scan speed of 10 mm/s for 106 seconds
3. Laser power 25%, pulse frequency of 700 Hz, scan speed 3 mm/s for 462 seconds

The laser-produced cross-section face is shown in Figure 3b. Roughness at the top of the cross section is from a prior test cut with the Ga FIB, and the empty space beneath the sample at the bottom of the cross section is from ablating through the full sample thickness. The laser ablation was set up to cut close but not into the ROI, so the anomalies identified by 3D XRM are not yet apparent. The secondary electron image of Figure 3b shows the grain structure appearing, and laser redeposited material coats the inner walls of the cut trench. Additional fine laser polishing could be done to achieve a smooth surface and enable EBSD directly after laser processing. However, EBSD was not required in this application.

Step 3 - Prepare: Just as with FIB milling, laser processing natively creates sloped sidewalls, although the physics mechanism differs. The fs-laser targeting accuracy can be as good as 2 μm for a surface target, while the amount of material in front of a buried target varies as a function of the target depth in combination with the slope angle of the cross-section face. The laser ablation was set to cut close to the buried anomalies but not through them, followed by Ga FIB milling to precisely target the cross-sectional plane and to prepare a final surface for analysis. An over-tilt was applied to the sample, and live imaging while FIB milling was performed until reaching the desired cross-sectional endpoint. Ion beam settings of 30 kV and 65 nA were chosen, rather than the highest ion beam current of 100 nA, to achieve fast milling while reducing the risk of overmilling or damaging the target site. After approximately 120 minutes, the cross section reached its final destination, successfully cutting into the target anomalies. The FE-SEM secondary electron images were acquired with accelerating voltage of 5 kV and 1 nA of beam current, and confirmed the anomalies identified by 3D XRM are particles with $\sim 10\ \mu\text{m}$ diameters (Figures 3c and 3d). Some of the crystallographic microstructure of the Fe matrix is also apparent. Since only basic EDS measurements are remaining to complete the analysis, additional fine FIB polishing to remove curtain artifacts was not performed, as it adds time without any benefit for the EDS analysis.

Step 4 - Analyze: A localized region of the cross section containing the $\sim 10\ \mu\text{m}$ -sized particles and their surrounding matrix was used for EDS mapping to analyze the elemental composition, as shown in Figure 4. The EDS was acquired at 15 kV accelerating voltage and 22 nA of beam current. The particles are found to be aluminum oxide, while the surrounding matrix is iron, as expected.

2 Access



3 Prepare

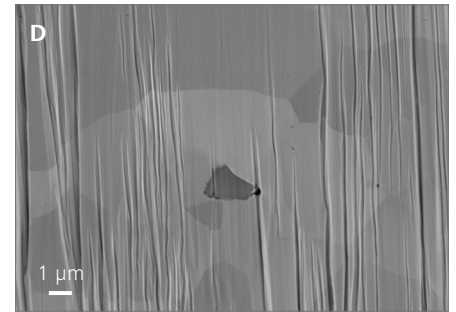
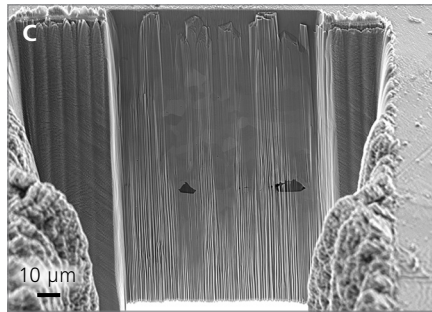


Figure 3 Within 10 minutes, fs-laser ablation has removed a huge volume of material at a location adjacent to the ROI (a,b), enabling access by the Ga FIB for preparing a precise cross section containing both buried anomalies (c, d).

4 Analyze

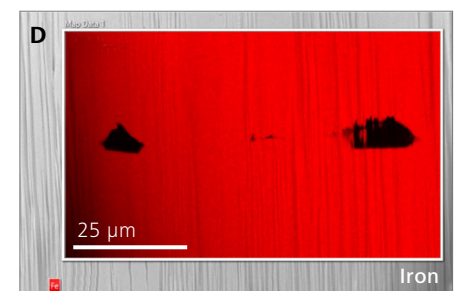
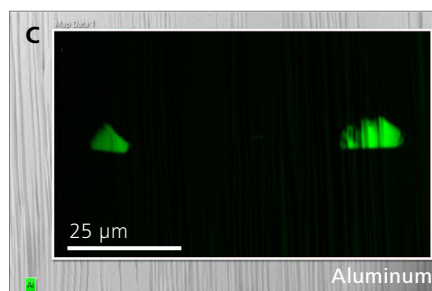
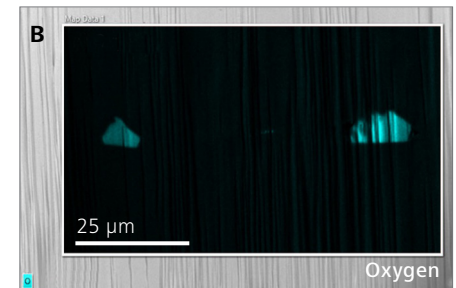
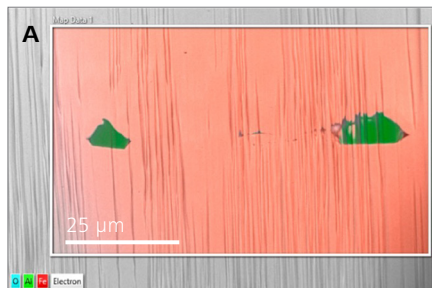


Figure 4 EDS mapping of the cross section through the two particles reveals their composition to be aluminum oxide.

Conclusions

This case study demonstrates an effective 4-step workflow to identify and selectively characterize anomalies on the order of a few microns within the bulk volume of a simple iron plate sample. By using 3D X-ray microscopy, correlative software, and FIB-SEM microscopy with integrated fs-laser milling, two sparse particles having roughly 10 µm diameters were found buried 100 µm deep within millimeter volumes of an otherwise homogenous material. Once identified and accessible, they were confirmed by EDS analysis to be aluminum oxide in an Fe matrix. The individual steps of the entire workflow, as shown in this case study, can be carried out at timescales that allow completing the full Cut2ROI workflow within a single day. In this example, the finding of aluminum oxide particles in the iron plate enabled discovery of the manufacturing process step that gave rise to these undesired particles.

The 4-step Cut2ROI workflow demonstrated here can be readily applied to other sample types that share the same challenge of needing to identify and characterize site-specific, subsurface features. Such applications include, for example, buried cracks or crack tips^[7], interfaces and defects between layered structures/coatings^[5], biological structures^[8], semiconductor package structures and defects^[3, 9], near-surface corrosion sites^[10], and particle or void distributions/ variations within composite materials^[11, 12] or electrochemical devices^[13, 14]. With continued adoption and applications development, additional novel applications of this Cut2ROI workflow will emerge, such as semiconductor package sample preparation for analysis by time domain reflectometry (TDR)^[15], or dense micropillar array fabrication as a material conservation approach to synchrotron sample preparation^[8].

References

- [1] ZEISS, *Xradia 630 Versa, Submicron 3D X-ray Imaging, Product Information V1.0*. 2023.
- [2] ZEISS Technical Note, *Resolution of a 3D X-ray Microscope: Defining Meaningful Resolution Parameters*. 2019.
- [3] Hartfield, C., et al., *Emerging Technologies for Advanced 3D Package Characterization to Enable the More-than-Moore Era*. ECS Transactions, 2022. **109**(2): p. 15-29.
- [4] HENRICH, L.F., L. CHEN, and A.J. BELL, *Simple technique for high-throughput marking of distinguishable micro-areas for microscopy*. 2016. **262**(1): p. 28-32.
- [5] Viswanathan, V. and L. Jiao, *Developments in Advanced Packaging Failure Analysis using Correlated X-Ray Microscopy and LaserFIB, in 2021 IEEE 23rd Electronics Packaging Technology Conference (EPTC)*. 2021. p. 80-84.
- [6] ZEISS, *ZEISS Crossbeam Family, Product Information V3.4 EN_42_011_091*. 2023.
- [7] Bale, H., *Investigation of stress corrosion cracking in CMSX-4 turbine blade alloys using Deep Learning assisted X-ray microscopy, in IUMAS-8: 8th Meeting of the International Union of Microbeam Analysis Societies*. 2023: Banff, CA.
- [8] Bosch, C., et al., *Femtosecond laser preparation of resin embedded samples for correlative microscopy workflows in life sciences*. Appl Phys Lett, 2023. **122**(14): p. 143701.
- [9] Kaestner, M., et al. *Novel workflow for high-resolution imaging of structures in advanced 3D and fan-out packages*. in *CSTIC*. 2019. China: IEEE.
- [10] Krebs, H.M., et al. *Time-Lapse Correlative 3D Imaging Applied to the Corrosion Study of AZ31 Mg Alloy in a Saline Environment*. in *Frontiers in Materials Processing, Applications, Research and Technology*. 2018. Singapore: Springer Singapore.
- [11] Li, J.-H., et al., *Rapid screening of Zr-containing particles from Chang'e-5 lunar soil samples for isotope geochronology: Technical roadmap for future study*. Geoscience Frontiers, 2022. **13**(3).
- [12] Schubert, T., et al., *Application of a Correlative fs-Laser Workflow for Fast and Easy Feature Access in Failure Analysis of Recycled Automotive Body Parts*. Microscopy and Microanalysis, 2022. **28**(S1): p. 868-870.
- [13] Vorauer, T., et al., *Impact of solid-electrolyte interphase reformation on capacity loss in silicon-based lithium-ion batteries*. Communications Materials, 2023. **4**(1).
- [14] Kelly, S., et al., *Non-destructive Correlative 3D Characterization of Nuclear Graphite: From the Micro-scale to the Nano-scale, in TMS 2021 150th Annual Meeting & Exhibition Supplemental Proceedings*. 2021. p. 553-562.
- [15] Viswanathan, V., et al. *Targeted Sample Preparation and Analysis of Advanced Packaging using Correlated X-Ray Microscopy and Laser FIB*. in *2022 IEEE CPMT Symposium Japan (ICSI)*. 2022. IEEE.